Alexandria Engineering Journal (2016) 55, 331–341

HOSTED BY

ELSEVIER

Alexandria University

Alexandria Engineering Journal

www.elsevier.com/locate/aej
www.sciencedirect.com

REVIEW

Influence of size, shape, type of nanoparticles, type and temperature of the base fluid on natural convection MHD of nanofluids

P. Sudarsana Reddy [a,*], **Ali J. Chamkha** [b]

[a] *Department of Mathematics, RGM College of Eng. & Tech, Nandyal 518501, AP, India*
[b] *Mechanical Engineering Department, Prince Mohammad Bin Fahd University, Al-Khobar 31952, Saudi Arabia*

Received 8 October 2015; revised 21 January 2016; accepted 27 January 2016
Available online 13 February 2016

KEYWORDS

Vertical cone;
Magnetic field;
Kerosene–Al_2O_3 and Water–TiO_2 nanofluids;
Size of nanoparticles (21 nm & 44 nm);
Spherical shape;
Finite element method

Abstract In this paper, we have presented MHD natural convection boundary layer flow, heat and mass transfer characteristics of nanofluid through porous media over a vertical cone influenced by different aspects of nanoparticles such as size, shape, type of nanoparticles and type of the base fluid and working temperature of base fluid. To increase the physical significance of the problem, we have taken dynamic viscosity and thermal conductivity as the functions of local volume fraction of nanoparticles. The drift-flux model of nanofluids, Brownian motion, thermophoresis, and enhancement ratio parameters are also considered in the present analysis. The influence of non-dimensional parameters such as magnetic field (M), buoyancy ratio parameter (Nr), conductivity parameter (Nc), viscosity parameter (Nv), Brownian motion parameter (Nb), thermophoresis parameter (Nt), Lewis number (Le) on velocity, temperature and volume fraction of nanoparticles in the boundary layer region is examined in detail. Furthermore the impact of these parameters on local Nusselt number (Nu_x) and enhancement ratio $\left(\frac{h_{nf}}{h_{bf}}\right)$ is also investigated. The results of present study reveal that significant natural convection heat transfer enhancement is noticed as the size of nanoparticles decreases. Moreover, type of the nanoparticles and type of the base fluid also influenced the natural convection heat transfer.

* Corresponding author.
E-mail addresses: suda1983@gmail.com (P. Sudarsana Reddy), achamkha@pmu.edu.sa (A.J. Chamkha).

Peer review under responsibility of Faculty of Engineering, Alexandria University.

http://dx.doi.org/10.1016/j.aej.2016.01.027

Nomenclature

A_1	density ratio (ρ_{bf}/ρ_{nf})
A_2	heat capacity ratio ($\rho c_{bf}/\rho c_{nf}$)
c	specific heat in constant pressure (J/kg K)
D_B	Brownian diffusion coefficient (m^2/s)
D_T	thermophoretic diffusion coefficient (m^2/s)
f	dimensionless stream function
g	gravitational acceleration (m/s^2)
jp	drift flux of nanoparticles
k	thermal conductivity coefficient (W/m K)
Kl	Porous parameter
Le	Lewis number
M	magnetic parameter
Nb	Brownian motion parameter
Nc	conductivity parameter
Nr	Buoyancy ratio
Nt	thermophoresis parameter
Nu	Nusselt number
Nv	viscosity parameter
P	pressure (Pa)
Pr	Prandtl number
Ra	Rayleigh number
S	Rescaled nanoparticle volume fraction
T	temperature (°C)
u	velocity component in x-direction (m/s)
v	velocity component in y-direction (m/s)
x	Cartesian coordinate in horizontal direction (m)
y	Cartesian coordinate in vertical direction (m)

Greek symbols

α	thermal diffusivity (m^2/s)
β	thermal expansion coefficient (1/K)
g	dimensionless distance
ρ	density (kg/m^3)
θ	non dimensional temperature
ϕ	volume fraction of nanoparticles
μ	thermal viscosity (kg s/m)
ψ	stream function

Subscript

bf	base fluid
nf	nanofluid
p	nanoparticles
∞	outside the boundary layer

Superscript

$'$	differentiation respect to η

Contents

1. Introduction

Natural convection flow, heat and mass transfer through porous medium over curved bodies has been attracted a much attention in recent years because of its enhanced physical and chemical properties. Nanofluids have wide range of applications in civil, mechanical and chemical engineering, thermal energy storage devices, heat exchangers, ground water systems, electronic cooling, boilers, heat loss from piping, crude oil extraction, etc. Spherical geometries, cones, cylinders, ellipses, wavy channels, and torus geometries are some examples of curved bodies. Good number of experimental and theoretical studies on transport phenomena over cylindrical bodies has been reported in the literature. All these studies are mainly focused on flow, heat and mass transfer characteristics of the commonly used base fluids such as water, ethylene glycol, and oil. A nanofluid is a fluid containing small volumetric quantities of nanometer-sized (smaller than 100 nm) particles, called nanoparticles or nanofibers. Nanofluids are the emerging composites consisting of nanoparticles or nanofibers dispersed in the conventional heat transfer base fluids such as water, ethylene glycol, toluene, and engine oil. The presence of nanoparticles in the base fluid may increase the thermal conductivity of the base fluid, and therefore it is predicted to improve the natural convection heat transfer of nanofluid with regard to the base fluid [1]. Khanafer and Vafai [2] have perceived that thermal conductivity and dynamic viscosity are very important thermo-physical properties of nanofluids and significantly influenced the convective heat transfer performance of nanofluids. In addition, they [2] also found that the thermal conductivity and dynamic viscosity of nanofluids are powerfully dependent on the nanoparticle volume fraction and rises as the values of nanoparticle volume fraction increase. Several authors, Kakac and Pramuanjaroenkij [3], Kleinstreuer and Feng [4], Ozerink et al. [5], Sundar et al. [6], and Wang and Mujumdar [7] have reported in their

experiment studies that the thermal conductivity and dynamic viscosity of nanofluids are functions of the size, shape, type of nanoparticles as well as the type of base fluid and working temperature of the base fluid. Furthermore, there are some other mechanisms which affect the thermo-physical properties of nanofluids such as the method of synthesis and sonication time. Moreover, Brownian motion and thermophoresis effects are the mass transfer mechanisms which also influence the convective heat transfer performance of nanofluids [8,9].

In his benchmark study, Buongiorno [10] has reported seven possible mechanisms associating nanofluid natural convection through moment of nanoparticles in the base fluid using scale analysis. These mechanisms are nanoparticle size, inertia, particle agglomeration, Magnus effect, volume fraction of the nanoparticle, Brownian motion and thermophoresis. Among all the mechanisms Brownian motion and thermophoresis are found to be very important. The thermophoresis acts against temperature gradient, so that, the particles move from the region of higher temperature to the region of lower temperature. Also, Brownian motion tends to move the particles from higher concentration areas to the lower concentration areas. Chandrasekhar et al. [11] have analyzed the dynamic viscosity and thermal conductivity of water–Al_2O_3 based nanofluid by dispersing spherical alumina powder nanoparticles of size 43 nm in the water, and then sonicated the nanofluid for 6 h. The dynamic viscosity was measured by using the Brookfield cone and plate viscometer. The thermal diffusivity was calculated with the help of hot wire method. In this experiment they [11] noticed that the values of dynamic viscosity and thermal conductivity both enhance as the values of nanoparticle volume fraction increase. Esfe et al. [12] analyzed the thermal conductivity and dynamic viscosity of MgO–water based nanofluids at room temperature. The spherical shape nanoparticles powder of size 40 nm was dispersed in the water using the ultrasonic waves. The dynamic viscosity and thermal conductivity are calculated by using Brookfield viscometer and hot wire method, respectively. The results reveals that, as the values of nanoparticles volume fraction enhance the values of dynamic viscosity and thermal conductivity also enhance. Agarwal et al. [13] have presented the impact of size of nanoparticles (21 nm, 44 nm) on thermal conductivity and the dynamic viscosity of kerosene–Al_2O_3 based nanofluid. The results suggested that when the size of nanoparticles is 21 nm the thermal conductivity and dynamic viscosity were higher than when the size of nanoparticles is 44 nm.

Nield and Kuznetsov [14] have extended the work of Buongiorno [10] to the natural convection boundary layer heat transfer of nanofluid through a porous medium. Kuznetsov and Nield [15] have discussed the influence of Brownian motion and thermophoresis on nanofluid natural convection boundary layer flow over a vertical plate. Aziz and Khan [16] have presented nanofluid natural convection boundary layer flow over a vertical plate subject to the convective boundary conditions. Chamkha et al. [17] studied the mixed convection MHD flow of a nanofluid past a stretching permeable surface in the presence of Brownian motion and thermophoresis effects. Rashidi et al. [18] discussed the dynamics of nanofluid from a non-linearly stretching sheet with transpiration using Homotopy simulation. Noghrehabadi and Behseresht [19] have analyzed how flow and heat transfer are affected by variable properties of nanofluid over a vertical cone saturated in a porous medium. Chamkha et al. [20] have discussed the mixed convection flow about vertical cone through porous medium saturated by a nanofluid with thermal radiation. In addition, Gorla et al. [21] have studied nanofluid natural convection boundary layer flow through porous medium over a vertical cone. Chamkha et al. [22] have investigated Non-Newtonian nanofluid natural convection flow over a cone through porous medium with uniform heat and volume fraction fluxes. Cheng [23] has presented double-diffusive natural convection heat and mass transfer of a porous media saturated nanofluid over a vertical cone. Behseresht et al. [24] have discussed heat and mass transfer characteristics of a nanofluid over a vertical cone using practical range of thermo-physical properties of nanofluids. Recently, Ghalambaz et al. [25] have analyzed the influence of nanoparticle diameter and concentration on natural convection heat and mass transfer of Al_2O_3–water based nanofluids over a vertical cone. Noghrehabadi et al. [26–28] have analyzed the natural convection of nanofluids over a stretching sheet by taking partial slip boundary conditions and prescribed constant wall temperature, vertical plate by taking heat generation/absorption and partial slip respectively. Teamah et al. [29] have presented augmentation of MHD natural convection heat transfer in square cavity by utilizing nanofluids by taking heat source into the account. Teamah [30] and Mohamed et al. [31] have analyzed boundary layer natural convective double-diffusive flow over rectangular enclosure by taking magnetic field and heat source. Qasim [32] has presented the effect of heat source/sink on heat and mass transfer analysis of Jeffery fluid past a stretching sheet. Das et al. [33] have reported the influence of thermal radiation on unsteady boundary layer flow of a nanofluid over a stretching sheet. Nandy et al. [34] have examined unsteady flow and heat transfer analysis of nanofluid over a permeable shrinking sheet with radiation. Das et al. [35] have discussed the impact of radiation on natural convection MHD flow of nanofluid over a moving vertical plate. Danial and Daniel [36] presented MHD flow over a stretching sheet through porous medium under the sway of buoyancy and radiation. Sudarsana Reddy and Suryanarayana Rao [37] have presented natural convection boundary layer heat and mass transfer characteristics of Al_2O_3–water and Ag–water nanofluids over a vertical cone.

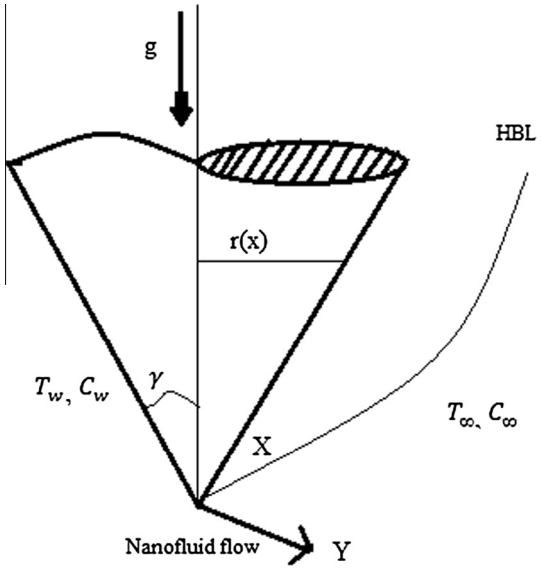

Figure 1 Physical model and coordinate system.

In all the abovementioned studies the boundary condition on the concentration of nanoparticles is taken as the analogous of the temperature. This means that the concentration of nanoparticles is actively controlled on the surface of the wall by taking a constant volume fraction. However, it is no longer possible to control the concentration of nanoparticles actively at the surface of the wall. This attracted many researchers to change the boundary condition at the surface of the wall. Kuznetsov and Neild [38] has presented natural convection boundary layer flow of a nanofluid past a vertical plate. In this paper they have proposed a new enhanced boundary condition for the volume fraction of nanoparticles at the surface of the wall. As the surface of the cone is impermeable, the nanoparticles cannot cross the surface of the cone, and hence, the mass flux of the nanoparticles at the surface is zero. Furthermore, the nanoparticles volume fraction on the boundary is passively controlled rather than actively controlled and this model is physically more realistic than the works published previously.

An inspection of the existing studies has suggested that, to the best of author's knowledge, no studies have been reported in the literature to study natural convection boundary layer flow, heat and mass transfer characteristics of a nanofluid through porous media over a vertical cone under the revised boundary conditions influenced by the size, shape, type of nanofluid as well as working temperature and type of the base fluid. Hence, the problem is addressed in this article. The objective of the present work was to solve this problem numerically using the finite element method and how the natural convection heat transfer of the nanofluids is affected by the different aspects such as size, shape, type of nanofluid as well as type and working temperature of the base fluid.

2. Mathematical formulation

Fig. 1 demonstrates a two-dimensional, study-state, electrically conducting heat and mass transfer boundary layer flow of nanofluid over a vertical cone. The coordinate system is chosen as the x-axis is coincident with the flow direction over the cone surface. It is assumed that T_w, and ϕ_w are the temperature and nanoparticle volume fraction at the surface of the cone ($y = 0$) and T_∞ and ϕ_∞ are the temperature and nanoparticle volume fraction of the ambient fluid, respectively. An external magnetic field of strength B_0 is applied in the direction of y-axis. Generally, the viscosity and thermal conductivity are considered as the function of temperature of the fluid. In the present analysis, we have considered nanofluid as the working fluid, and viscosity and thermal conductivity are functions of volume fraction of nanoparticles. By considering the works [38] and Buongiorno [10] and applying the usual boundary layer approximations, the governing equations describing the steady-state conservation of mass, momentum, energy as well as conservation of the mass nanoparticles in the presence of magnetic parameter and other important parameters take the following form:

$$\frac{\partial(ru)}{\partial x}+\frac{\partial(rv)}{\partial y}=0 \tag{1}$$

$$\left(u_{nf}\frac{\partial u_{nf}}{\partial x}+v_{nf}\frac{\partial u_{nf}}{\partial y}\right)=\frac{1}{\rho_{nf}}\frac{\partial}{\partial y}\left(\mu_{nf}(\phi)\frac{\partial u_{nf}}{\partial y}\right)+\frac{g}{\rho_{nf}}\left[\beta_{bf}\rho_{bf,\infty}(\phi-\phi_\infty)(T_{nf}-T_\infty)-(\rho-\rho_{bf,\infty}(\phi-\phi_\infty)\right]Cos\gamma-\frac{\mu_{nf}}{\rho_{nf}}\frac{1}{K}u_{nf}-\frac{\sigma B_0^2}{\rho_{nf}}u_{nf} \tag{2}$$

$$\left(u_{nf}\frac{\partial T_{nf}}{\partial x}+v_{nf}\frac{\partial T_{nf}}{\partial y}\right)=\frac{1}{(\rho c)_{nf}}\frac{\partial}{\partial y}\left(k_{nf}(\phi)\frac{\partial T_{nf}}{\partial y}\right)+(\rho c)_p\left[D_B\frac{\partial\phi}{\partial y}.\frac{\partial T_{nf}}{\partial y}+\left(\frac{D_T}{T_\infty}\right)\left(\frac{\partial T_{nf}}{\partial y}\right)^2\right] \tag{3}$$

$$u_{nf}\frac{\partial\phi}{\partial x}+v_{nf}\frac{\partial\phi}{\partial y}=D_B\frac{\partial^2\phi}{\partial y^2}+\left(\frac{D_T}{T_\infty}\right)\frac{\partial^2 T_{nf}}{\partial y^2} \tag{4}$$

The boundary conditions based on the problem description are as follows:

$$u_{nf}=0,\quad v_{nf}=0,\quad T_{nf}=T_w,\quad j_p=0\quad \text{at } y=0 \tag{5}$$

$$u_{nf}\to 0,\quad T_{nf}\to T_\infty,\quad \phi\to\phi_\infty\quad \text{at } y\to\infty \tag{6}$$

where $j_p=-D_B\nabla\phi-D_T\frac{\nabla T}{T}$, is the drift-flux model of nanoparticles. Furthermore, the concentration boundary condition at $y = 0$ is taken as $j_p = 0$. This is because of the fact that, the nanoparticles cannot cross the surface of the cone as the surface of the cone is impermeable.

The continuity Eq. (1) is satisfied by introducing a stream function ψ as

$$u=\frac{1}{r}\frac{\partial\psi}{\partial y},\quad v=-\frac{1}{r}\frac{\partial\psi}{\partial x} \tag{7}$$

The following similarity transformations are introduced to simplify the mathematical analysis of the problem:

$$\eta=\frac{y}{x}Ra_x^{1/4},\quad f(\eta)=\frac{\psi}{\alpha_m Ra_x^{1/4}},$$
$$\theta(\eta)=\frac{T_{nf}-T_\infty}{T_w-T_\infty},\quad S(\eta)=\frac{\phi-\phi_\infty}{\phi_\infty} \tag{8}$$

where Ra_x is the local Rayleigh number and is defined as

$$Ra_x=\frac{g\beta_{bf}\rho_{bf}(T_{nf}-T_\infty)x^3Cos\gamma}{\mu_{bf}\alpha_{bf}} \tag{9}$$

and r can be approximated by the local radius of the cone, if the thermal boundary layer is thin, and is related to the x coordinate by $r = x\ sin\gamma$.

The thermal conductivity and dynamic viscosity of nanofluids are the linear function of nanoparticle volume fraction and are defined as follows [10,39]:

$$\frac{k_{nf}}{k_{bf}}=1+Nc\,\phi,\quad \frac{\mu_{nf}}{\mu_{bf}}=1+Nv\,\phi \tag{10}$$

Now, with the support of similarity variables (8) and (10) the governing non-linear partial differential Eqs. (2)–(4) together with boundary conditions (5) and (6) take the following form:

$$A_1[1+Nv\phi_\infty(1+S)f'''+A_1Nv\phi_\infty f''S'+\frac{1}{Pr}\left[\frac{3}{4}f'f''-\frac{1}{2}f'f'\right]+A_1[(1-\phi_\infty)\theta-NrS]-K1f'-A_1Mf'=0 \quad (11)$$

$$A_2[1+Nc\phi_\infty(1+S)\theta''+A_2Nc\phi_\infty S'\theta'+\frac{3}{4}f\theta'+NbS'\theta'+Nt(\theta')^2=0 \quad (12)$$

$$S''+\frac{3}{4}LefS'+\frac{Nt}{Nb}\theta''=0 \quad (13)$$

The transformed boundary conditions are

$$\eta=0,\quad f=0,\quad f'=1,\quad \theta=1,\quad NbS'+Nt\theta'=0.$$
$$\eta\to\infty,\quad f'=0,\quad \theta=0,\quad S=0. \quad (14)$$

where prime denotes differentiation with respect to η. In some practical situations the nanofluid flow simulation is strongly influenced by the thermophoresis force, so we could not eliminate this term from the zero mass flux boundary condition of nanoparticles $NbS'+Nt\theta'=0$. In these cases we have to adjust the nanoparticles volume fraction at the surface of the cone, but it leads to the negative value for the volume fraction of nanoparticles. In this case, the zero mass flux boundary condition of nanoparticles at the surface is replaced with the zero volume fraction of nanoparticles (i.e. $S'=-1$).

The significant thermo-physical parameters dictating the flow dynamics are defined by

$$Nr=\frac{(\rho_p-\rho_{bf})\phi_\infty}{\beta_{bf}\rho_{bf}(T_w-T_\infty)},\quad A_1=\frac{\rho_{bf}}{\rho_{nf}},\quad A_2=\frac{(\rho c)_{bf}}{(\rho c)_{nf}},$$
$$Pr=\frac{\mu_{bf}}{\rho_{bf}\alpha_{bf}},\quad K1=\frac{x^2}{KRa_x^{1/2}},$$
$$M=\frac{\sigma\beta_o^2x^2}{Ra_x^{1/2}\mu_{bf}},\quad Nb=\frac{(\rho c)_pD_B\phi_\infty}{(\rho c)_{nf}\alpha_{bf}},$$
$$Nt=\frac{(\rho c)_pD_T(T_w-T_\infty)}{(\rho c)_{nf}\alpha_{bf}T_\infty},\quad Le=\frac{\alpha_{bf}}{D_B}.$$

Quantities of practical interest in this problem are the local Nusselt number Nu_x, and enhancement ratio $\left(\frac{h_{nf}}{h_{bf}}\right)$, and these are defined as

$$Nu_x=\frac{h_{nf}w}{h_{bf}}\theta'_{nf}(0)Ra_x^{\frac{1}{4}},\quad \frac{h_{nf}}{h_{bf}}=(1+\phi_\infty Nc(1+S(0)))\frac{\theta'_{nf}(0)}{\theta'_{bf}(0)}.$$

The set of ordinary differential Eqs. (11)–(13) are highly non-linear, and therefore cannot be solved analytically. The finite-element method [43–45] has been implemented to solve these non-linear equations. The very important aspect in this numerical procedure is to select an approximate finite value of η_∞. So, in order to estimate the relevant value of η_∞, the solution process has been started with an initial value of $\eta_\infty=4$, and then the Eqs. (11)–(13) are solved together with boundary conditions (14). We have updated the value of η_∞ and the solution process is continued until the results are not affected with further values of η_∞ The choice of $\eta_{max}=4$, $\eta_{max}=16$ and $\eta_{max}=6$ for velocity, temperature and concentration has confirmed that all the numerical solutions approach to the asymptotic values at the free stream conditions.

3. Numerical method of solution

The finite-element method (FEM) is such a powerful method for solving ordinary differential equations and partial differential equations. The basic idea of this method is dividing the whole domain into smaller elements of finite dimensions called finite elements. This method is such a good numerical method in modern engineering analysis, and it can be applied for solving integral equations including heat transfer, fluid mechanics, chemical processing, electrical systems, and many other fields. The steps involved in the finite-element are as follows:

(i) Finite-element discretization.
(ii) Generation of the element equations.
(iii) Assembly of element equations.
(iv) Imposition of boundary conditions.
(v) Solution of assembled equations.

The assembled equations so obtained can be solved by any of the numerical techniques, namely, the Gauss elimination method, LU decomposition method, etc. An important consideration is the shape functions which are employed to approximate actual functions.

4. Results and discussion

The system of Eqs. (11)–(13) together with the boundary conditions (14) are solved for different values of the parameters that describe the flow characteristics and the results are illustrated graphically and in tabular form. Numerical solution of the problem has been carried out for fixed $\phi_\infty=3\%$, and variations in size, shape, type of nanofluids and type of base fluid, working temperature of the base fluid are shown in Table 1. In the present study, we have taken two types of nanofluids (Al_2O_3, TiO_2), two sizes (21 nm, 44 nm), spherical shape of nanoparticle, two base fluids (water, kerosene), and working temperature of base fluid (25 °C), as listed in Table 2 (case 1 & case 2). The comparison with previously published work is made and shown in Fig. 2. The thermo-physical properties of water and nanoparticles is shown in Table 3. The velocity, temperature and volume fraction distributions of nanoparticles are calculated for various values of the parameters entered into the problem and are presented graphically in Figs. 3–18.

The effect of magnetic field parameter (M) on the boundary layer flow, heat and mass transfer is depicted in Figs. 3–5 for the two cases C1 (case 1) and C2 (case 2). The velocity profiles impede throughout the boundary layer with the increase in the strength of magnetic parameter for both cases. This is due to the fact that the presence of a magnetic field in the flow creates a force known as the Lorentz force which acts as a retarding force and consequently, the momentum boundary layer thickness decelerates throughout the flow region (Fig. 3). We define the thermal energy as the additional force which drags the nanofluid from the influence of the magnetic field. This additional force increases the thickness of the thermal boundary layer, so that the temperature profile enriches with rise in M and is higher in C2 than in C1 (Fig. 4). From Fig. 5, we have noticed that as the value of M increases, the volume fraction of nanoparticles distributions is also enriched in the flow regime in the both nanofluids.

Table 1 Thermo-physical properties of water and kerosene [40,41].

Type	Temperature (°C)	Density (kg/m^3)	Specific heat capacity (J/kg K)	Volume thermal expansion $(1/K) \cdot 10^{-4}$	Dynamic viscosity (Pa s)	Thermal conductivity (W/m^2 K)	Prandtl
Water	25	997.05	4181.4	2.253	8.93	0.606	6.161
Kerosene	25	790	2010.0	10.00	14.11	0.101	28.10

Table 2 The non-dimensional parameters for different samples of nanofluids.

Case	Temperature	Type	Base fluid	Size (nm)	Shape	ρ_{bf}/ρ_{nf}	$(\rho c)_{bf}/(\rho c)_{nf}$
1 (C1)	25	TiO_2	Water	21	Spherical	0.9108	1.0089
2 (C2)	25	Al_2O_3	Kerosene	44	Spherical	0.8929	0.9731

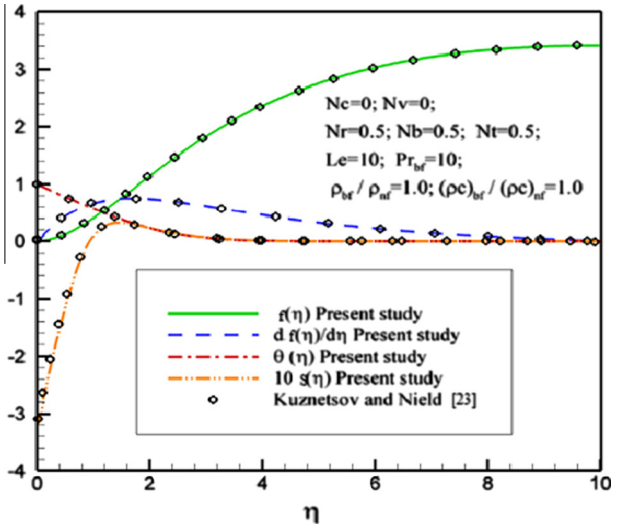

Figure 2 Comparison with previously published work.

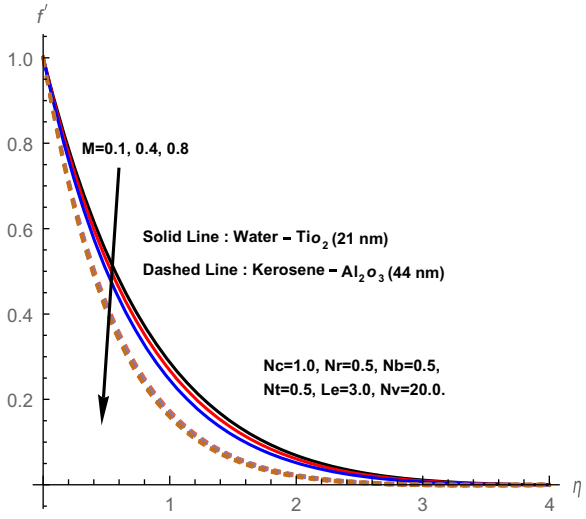

Figure 3 Effect of M on velocity profiles.

Figs. 6 and 7 depict velocity (f') and temperature (θ) distributions for different values of the buoyancy ratio parameter (Nr). From Fig. 6 we have noticed retardation in the thickness of hydrodynamic boundary layer in both the cases C1 and C2 with the higher values of (Nr). The temperature profiles of the both fluids increase with increasing values of buoyancy ratio parameter (Nr). This is from the reality that higher values of buoyancy ratio parameter enhance the temperature of the both fluids, so that thermal boundary layer thickness is increased and is higher in C2 than in C1 (Fig. 7). Figs. 8–10 illustrate the influence of variable viscosity parameter (Nv) on the dimensionless velocity (f'), temperature (θ) and volume fraction (S) distributions of nanoparticles for two cases C1 and C2. Higher values of (Nv) mean more dependency of dynamic viscosity on volume fraction of nanoparticles. From Fig. 8, we noticed that a rise in variable viscosity parameter (Nv) enriches the velocity profiles in the boundary layer regime in the both cases. It is observed that the temperature distributions retard with increasing values of Nv (Fig. 9). This is because of the fact that the thickness of the thermal boundary layer is reduced as the values of Nv increase. However, the nanoparticle volume fraction profiles enrich with the higher values of Nv in both the cases C1 and C2 (Fig. 10).

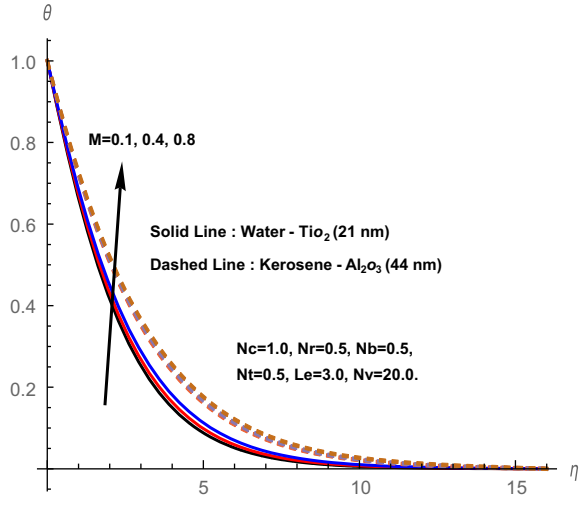

Figure 4 Effect of M on temperature profiles.

The non-dimensional distributions of velocity (f'), temperature (θ) and nanoparticles volume fraction (S) are depicted in Figs. 11–13 for different values of variable thermal

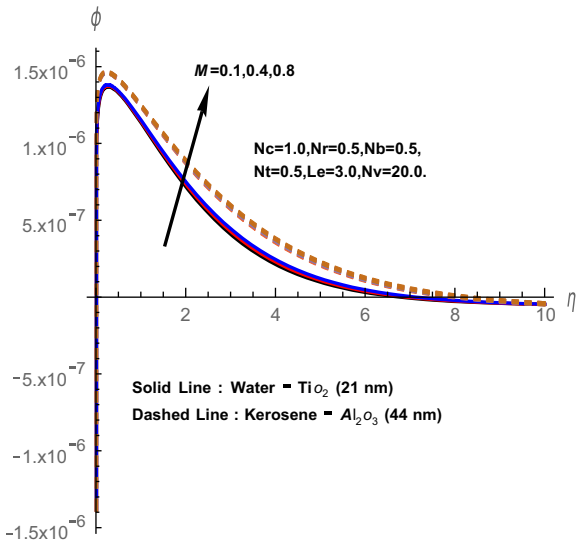

Figure 5 Effect of M on concentration profiles.

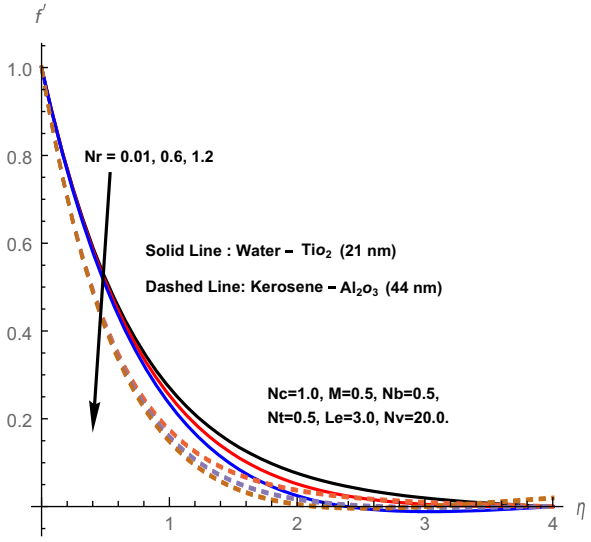

Figure 6 Effect of Nr on velocity profiles.

conductivity parameter (Nc). It is confirmed from Figs. 11 and 12 that both hydrodynamic and thermal boundary layer thicknesses are enriched in the two cases C1 and C2 with the improving values of (Nc). This is because of the reality that the thermal conductivity of nanofluid increases near the cone surface as the values of (Nc) increase, so that the temperature profiles elevate. Temperature of the nanofluid is increasing means the buoyancy force is increasing; consequently, the velocity of the nanofluid enhances in flow regime. It is evident from Fig. 12 that there is significant heat transfer enhancement in the boundary layer regime when the size of nanoparticles reduces. The magnitude of nanoparticle volume fraction concentration profiles also elevates with the higher values of (Nc) as shown in Fig. 13.

Variation of non-dimensional temperature and volume fraction distributions for different values of thermophoretic parameter (Nt) for the cases C1 and C2 is depicted in Figs. 14 and 15. It is noticed from these figures that both temperature

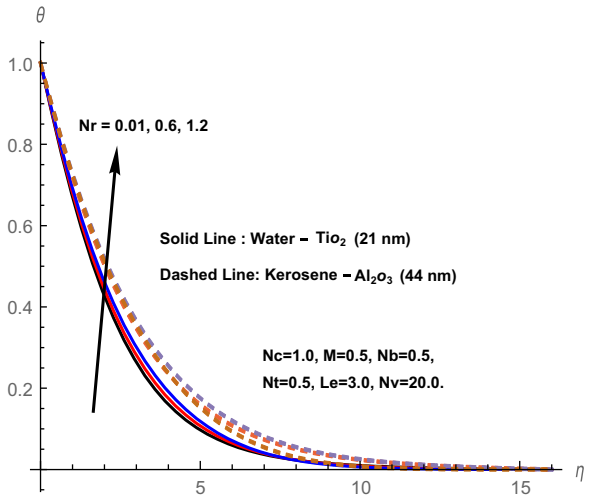

Figure 7 Effect of Nr on temperature profiles.

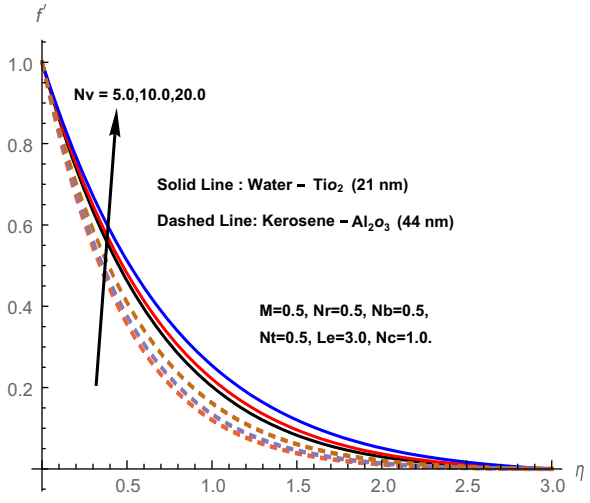

Figure 8 Effect of Nv on velocity profiles.

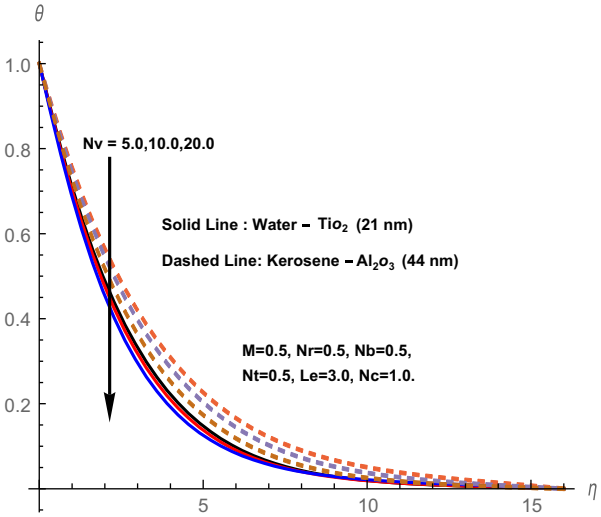

Figure 9 Effect of Nv on temperature profiles.

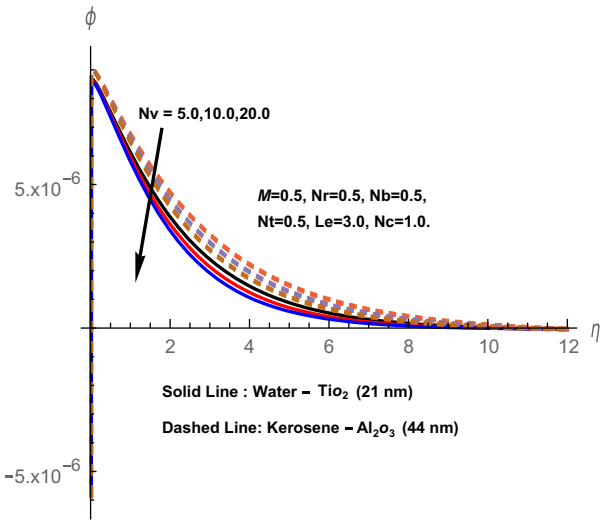

Figure 10 Effect of *Nv* on concentration profiles.

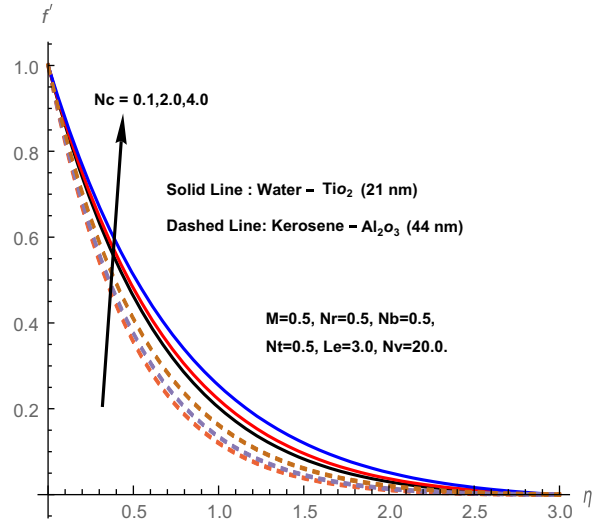

Figure 11 Effect of *Nc* on velocity profiles.

and concentration profiles elevate in the boundary layer region with the higher values of thermophoretic parameter (*Nt*) and are more in the case C2 than in the case C1. This is from the reality that particles near the hot surface create thermophoretic force; this force enhances the temperature and concentration of the fluid in the boundary layer region.

The effect of Brownian motion parameter (*Nb*) on temperature and nanoparticle volume fraction profiles is illustrated in Figs. 16 and 17 for C1 and C2 cases. Brownian motion is the random motion of suspended nanoparticles in the base fluid and is more influenced by its fast moving atoms or molecules in the base fluid. It is worth to mention that Brownian motion is related to the size of nanoparticles and is often in the form of agglomerates and/or aggregates. It is noticed that, with the increasing values of Brownian motion parameter (*Nb*) temperature as well as volume fraction of nanoparticle profiles deteriorates in the boundary layer regime and this reduction is more in C1 than the C2. The impact of the Lewis number (*Le*) on nanoparticle volume fraction profiles is plotted in Fig. 18. It is observed that nanoparticle volume fraction distributions decelerate with the increasing values of the Lewis

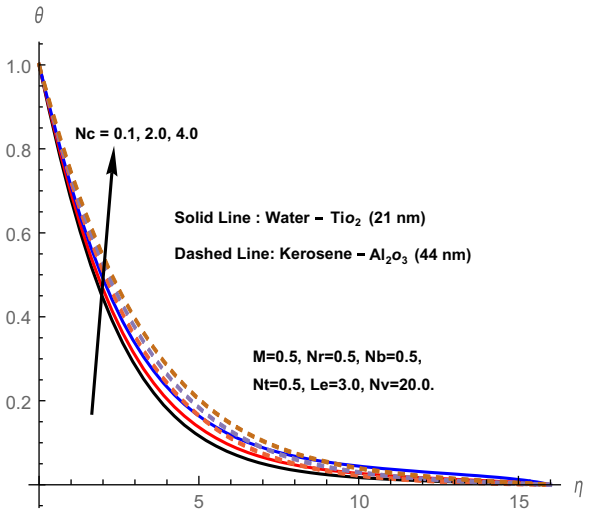

Figure 12 Effect of *Nc* on temperature profiles.

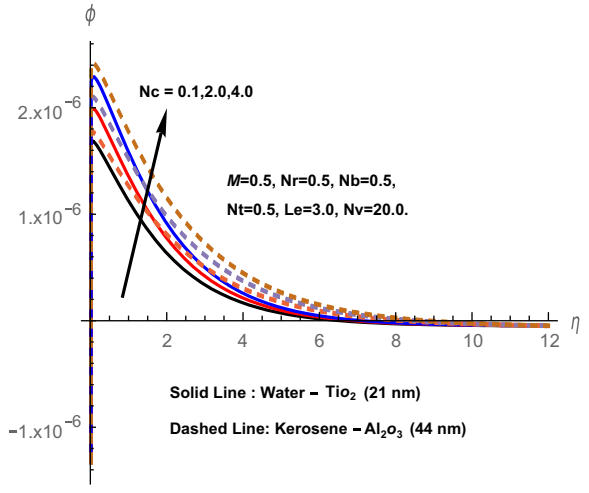

Figure 13 Effect of *Nc* on concentration profiles.

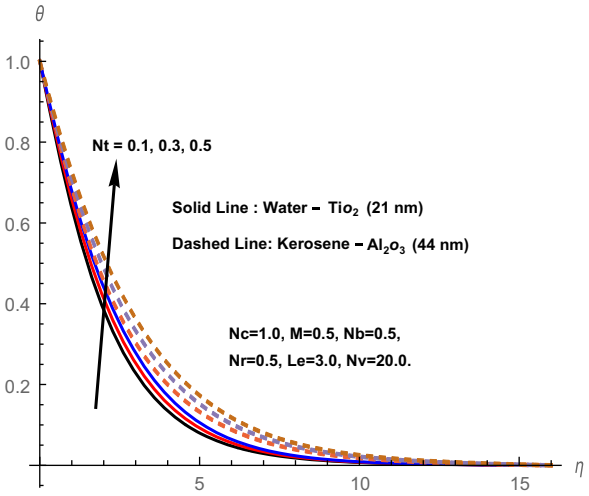

Figure 14 Effect of *Nt* on temperature profiles.

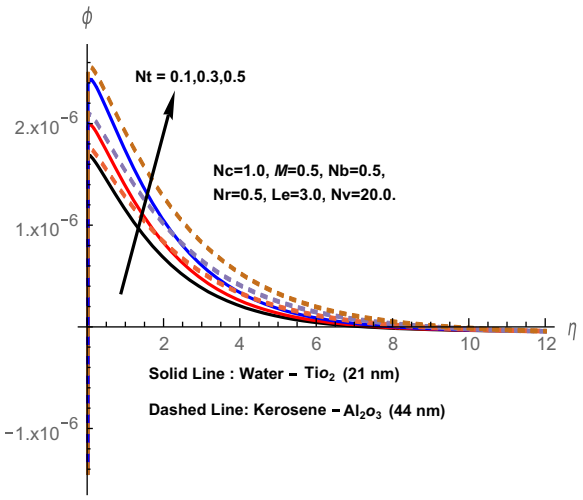

Figure 15 Effect of *Nt* on concentration profiles.

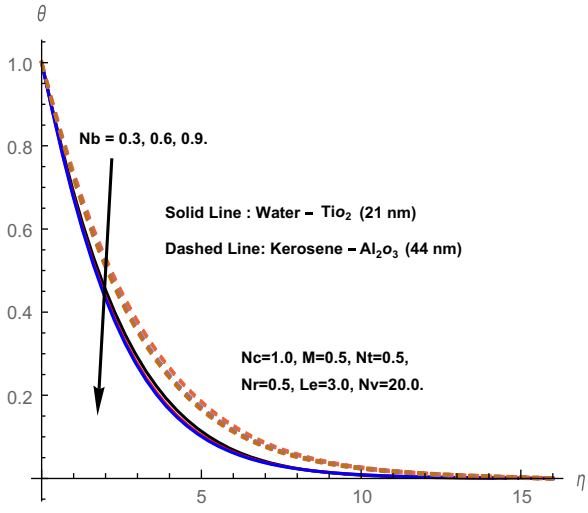

Figure 16 Effect of *Nb* on temperature profiles.

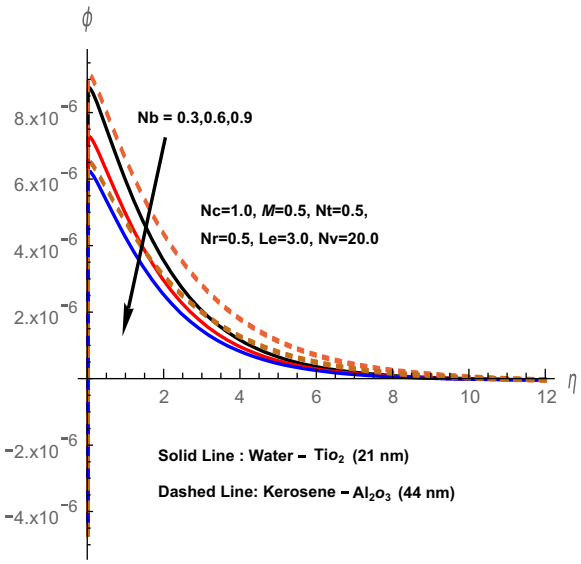

Figure 17 Effect of *Nb* on concentration profiles.

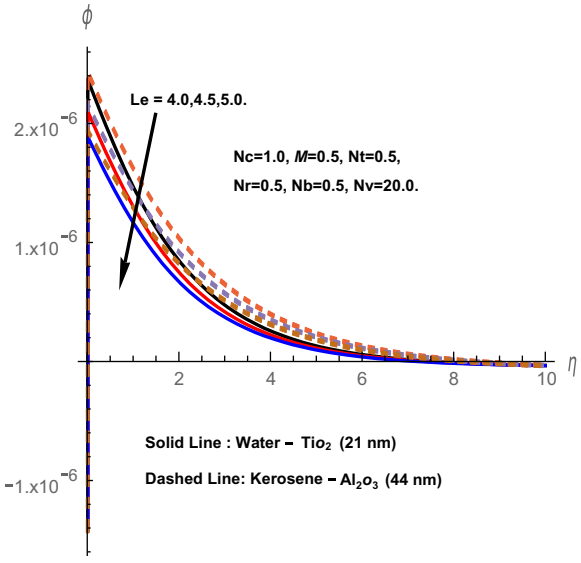

Figure 18 Effect of *Le* on concentration profiles.

number in the entire boundary layer region. By definition, the Lewis number represents the ratio of the thermal diffusivity to the mass diffusivity. Increasing the Lewis number means a higher thermal diffusivity and a lower mass diffusivity, and this produces thinner concentration boundary layer.

The rates of heat transfer $(-\theta'(0))$ and the enhancement ratio $(\frac{h_{nf}}{h_{bf}})$ for different values of the non-dimensional parameters are exhibited in Table 4. It is evident from this table that the rates of heat transfer and enhancement ratio both depreciate with the higher values of magnetic field parameter (M) in both the cases C1 and C2. The Nusselt number (Nu_x) and the enhancement ratio both decelerate with the improving values of thermophoresis parameter (Nt) in both the nanofluids. It is clear from this table that as the magnitude of Brownian motion parameter (Nb) increases the heat transfer rates and enhancement ratio also increase in both the nanofluids. The Nusselt number (Nu_x) and the enhancement ratio both decrease with the higher values of thermal conductivity parameter (Nc) for both the cases C1 and C2. However, exact reverse trend is noticed in the rates of heat transfer and enhancement ratio parameter with the increasing values of thermal conductivity parameter (Nc).

Table 3 Thermo-physical properties of water and nanoparticles [42].

Nanofluid	$\rho\left(\frac{kg}{m^3}\right)$	$C_p\left(\frac{J}{kg\ K}\right)$	$k\left(\frac{W}{mK}\right)$	$\beta(10^{-6}\left(\frac{1}{K}\right))$	$\alpha\left(\frac{m^2}{s}\right)$
Alumina (Al_2O_3)	3970	765	40	17.4	1.310
Titanium oxide (TiO_2)	4250	686.2	8.9538	12.2	0.286

Table 4 The Nusselt number $(-\theta'(0))$ and enhancement ratio $\left(\frac{h_{nf}}{h_{bf}}\right)$ values for different values of M, Nt, Nb, Nc, Nv.

Parameter					$-\theta'(0)$		$\left(\frac{h_{nf}}{h_{bf}}\right)$	
M	Nt	Nb	Nc	Nv	Al_2O_3	TiO_2	Al_2O_3	TiO_2
0.1	0.5	0.5	1.0	20	0.301337	0.363297	1.129417	1.196095
0.4	0.5	0.5	1.0	20	0.297327	0.352582	1.118166	1.181737
0.8	0.5	0.5	1.0	20	0.291259	0.339089	1.104735	1.163435
0.5	0.1	0.5	1.0	20	0.340654	0.394980	1.161093	1.218679
0.5	0.3	0.5	1.0	20	0.326877	0.369790	1.135148	1.191977
0.5	0.5	0.5	1.0	20	0.293388	0.345664	1.110992	1.166403
0.5	0.5	0.3	1.0	20	0.282952	0.334240	1.201234	1.154294
0.5	0.5	0.6	1.0	20	0.295884	0.348280	1.213637	1.169177
0.5	0.5	0.9	1.0	20	0.312587	0.352406	1.217906	1.173550
0.5	0.5	0.5	0.1	20	0.323644	0.346928	1.173312	1.130191
0.5	0.5	0.5	2.0	20	0.295129	0.327291	1.153423	1.105841
0.5	0.5	0.5	4.0	20	0.269809	0.307113	1.134564	1.080820
0.5	0.5	0.5	1.0	5.0	0.261236	0.312242	1.121895	1.184745
0.5	0.5	0.5	1.0	10	0.273659	0.321967	1.137203	1.196726
0.5	0.5	0.5	1.0	20	0.293243	0.337473	1.161334	1.215834

5. Conclusion

The natural convection boundary layer heat and mass transfer characteristics of nanofluids over a vertical cone is analyzed by taking two types of nanoparticles, two sizes of nanoparticles, spherical shape of nanoparticles, two base fluids and its working temperature and the influence of magnetic field. Three important affective parameters dynamic viscosity, thermal conductivity and enhancement ratio are considered in this problem. The new enhanced zero mass flux boundary condition of nanoparticles at the surface of the cone was effectively utilized. The similarity transformation approach was applied to convert the governing equations into the set of ordinary differential equations. These equations are solved using finite element method and results are shown in graphically as well as in tabular form. The following conclusions are made in the present study:

(i) Figs. 12 and 14 clearly indicate that there is significant heat transfer enhancement in the boundary layer regime as the size of nanoparticles decreases. Therefore, the nanoparticles with smaller sizes influenced the heat transfer enhancement of the fluid than the nanoparticles with higher sizes.

(ii) Type of nanoparticles also plays very important role in natural convection heat transfer enhancement. It is evident from Fig. 9 that the natural convection heat transfer retardation is more when TiO_2 nanoparticles are dispersed in water than the Al_2O_3 nanoparticles that are dispersed in kerosene.

(iii) The heat transfer enhancement is higher in kerosene–Al_2O_3 (44 nm) than in the water–TiO_2 (21 nm) with the increasing values of (Nc).

(iv) The thickness of the hydrodynamic boundary layer for water–TiO_2 (21 nm) is significantly lower than that for the kerosene–Al_2O_3 (44 nm) with higher values of (Nv).

(v) The thickness of the thermal boundary layer for water–TiO_2 (21 nm) is significantly higher than that for the kerosene–Al_2O_3 (44 nm) with higher values of (Nv).

(vi) Both temperature and concentration profiles elevate as the values of thermophoretic parameter (Nt) increase in the boundary layer regime.

Acknowledgment

The authors are very much thankful to the reviewers for their decent suggestions and observations to improve the quality of the manuscript.

References

[1] S.K. Das, S. Choi, W. Yu, T. Pradeep, Nanofluids: Science and Technology, Wiley Interscience, New Jersey, 2007.
[2] K. Khanafer, K. Vafai, A critical synthesis of thermophysical characteristics of nanofluids, Int. J. Heat Mass Transfer 54 (2011) 4410–4428.
[3] S. Kakac, A. Pramuanjaroenkij, Review of convective heat transfer enhancement with nanofluids, Int. J. Heat Mass Transfer 52 (2009) 3187–3196.
[4] C. Kleinstreuer, Y. Feng, Experimental and theoretical studies of nanofluid thermal conductivity enhancement: a review, Nanoscale Res. Lett. 6 (2011) 229.
[5] S. Ozerinc, S. Kakac, A. Yazıcıoglu, Enhanced thermal conductivity of nanofluids: a state-of- the-art review, Microfluid. Nanofluid. 8 (2010) 145–170.
[6] L.S. Sundar, K.V. Sharma, M.T. Naik, M.K. Singh, Empirical and theoretical correlations on viscosity of nanofluids: a review, Renew. Sustain. Energy Rev. 25 (2013) 670–686.
[7] X.-Q. Wang, A.S. Mujumdar, Heat transfer characteristics of nanofluids: a review, Int. J. Therm. Sci. 46 (2007) 1–19.
[8] A.V. Kuznetsov, D.A. Nield, Natural convective boundary-layer flow of a nanofluid past a vertical plate, Int. J. Therm. Sci. 49 (2010) 243–247.
[9] E. Abu-Nada, A.J. Chamkha, Mixed convection flow in a lid-driven inclined square enclosure filled with a nanofluid, Eur. J. Mech.-B/Fluids 29 (2010) 472–482.
[10] J. Buongiorno, Convective transport in nanofluids, J. Heat Transfer 128 (2006) 240–250.
[11] M. Chandrasekar, S. Suresh, A. Chandra Bose, Experimental investigations and theoretical determination of thermal

conductivity and viscosity of Al_2O_3/water nanofluid, Exp. Therm. Fluid Sci. 34 (2010) 210–216.
[12] H.M. Esfe, S. Saedodin, M. Mahmoodi, Experimental studies on the convective heat transfer performance and thermophysical properties of MgO–water nanofluid under turbulent flow, Exp. Therm. Fluid Sci. 52 (2014) 68–78.
[13] D.K. Agarwal, A. Vaidyanathan, S. Sunil Kumar, Synthesis and characterization of kerosene–alumina nanofluids, Appl. Therm. Eng. 60 (2013) 275–284.
[14] D.A. Nield, A.V. Kuznetsov, The Cheng – Minkowycz problem for natural convection boundary-layer flow in a porous medium saturated by a nanofluid, Int. J. Heat Mass Transfer 52 (2009) 5792–5795.
[15] A.V. Kuznetsov, D.A. Nield, Natural convective boundary-layer flow of a nanofluid past a vertical plate, Int. J. Therm. Sci. 49 (2010) 243–247.
[16] A. Aziz, W.A. Khan, Natural convective boundary layer flow of a nanofluid past a convectively heated vertical plate, Int. J. Therm. Sci. 52 (2012) 83–90.
[17] A.J. Chamkha, A.M. Aly, H. Al-Mudhaf, Laminar MHD mixed convection flow of a nanofluid along a stretching permeable surface in the presence of heat generation or absorption effects, Int. J. Micros. Nanos. Therm. Fluid Transp. Phenom. 2 (2011) 51–70.
[18] M.M. Rashidi, N. Freidoonimehr, A. Hosseini, O. Anwar Bég, T.K. Hung, Homotopy simulation of nanofluid dynamics from a non-linearly stretching isothermal permeable sheet with transpiration, Meccanica 49 (2014) 469–482.
[19] A. Noghrehabadi, A. Behseresht, Flow and heat transfer affected by variable properties of nanofluids in natural-convection over a vertical cone in porous media, Comput. Fluids 88 (2013) 313–325.
[20] A.J. Chamkha, S. Abbasbandy, A.M. Rashad, K. Vajravelu, Radiation effects on mixed convection about a cone embedded in a porous medium filled with a nanofluid, Meccanica 48 (2013) 275–285.
[21] R.S.R. Gorla, A.J. Chamkha, V. Ghodeswar, Natural convective boundary layer flow over a vertical cone embedded in a porous medium saturated with a nanofluid, J. Nanofluids 3 (2014) 65–71.
[22] A.J. Chamkha, S. Abbasbandy, A.M. Rashad, Non-Darcy natural convection flow of non-Newtonian nanofluid over a cone saturated in a porous medium with uniform heat and volume fraction fluxes, Int. J. Numer. Methods Heat Fluid Flow 25 (2015) 422–437.
[23] C.Y. Cheng, Double-diffusive natural convection from a vertical cone in a porous medium saturated with a nanofluid, J. Chin. Soc. Mech. Eng. 34 (2013) 401–409.
[24] A. Behseresht, A. Nogrehabadi, M. Ghalambaz, Natural-convection heat and mass transfer from a vertical cone in porous media filled with nanofluids using practical ranges of nanofluids thermo-physical properties, Chem. Eng. Res. Des. 92 (2014) 447–452.
[25] M. Ghalambaz, A. Behseresht, J. Behseresht, A.J. Chamkha, Effect of nanoparticle diameter and concentration on natural convection in Al_2O_3–water nanofluids considering variable thermal conductivity around a vertical cone in porous media, Adv. Powder Technol. 26 (2015) 224–235.
[26] A. Noghrehabadi, A. Behseresht, M. Ghalambaz, Natural convection of nanofluid over vertical plate embedded in porous medium: prescribed surface heat flux, Appl. Math. Mech. 34 (2013) 669–686.
[27] A. Noghrehabadi, R. Pourrajab, M. Ghalambaz, Effect of partial slip boundary condition on the flow and heat transfer of nanofluids past stretching sheet prescribed constant wall temperature, Int. J. Therm. Sci. 54 (2013) 253–261.
[28] A. Noghrehabadi, M.R. Saffarian, R. Pourrajab, M. Ghalambaz, Entropy analysis for nanofluid flow over a stretching sheet in the presence of heat generation/absorption and partial slip, J. Mech. Sci. Technol. 27 (2013) 927–937.
[29] M.A. Teamah, W.M. El-Maghlany, Augmentation of natural convection heat transfer in square cavity by utilizing nanofluids in the presences of magnetic field and heat source, Int. J. Therm. Sci. 58 (2012) 130–142.
[30] M.A. Teamah, Numerical simulation of double diffusive natural convection in rectangular enclosure in the presences of magnetic field and heat source, Int. J. Therm. Sci. 47 (2008) 237–248.
[31] Mohamed A. Teamah, Ahmad F. Elsafty, Enass Z. Massoud, Numerical simulation of double-diffusive natural convective flow in an inclined rectangular enclosure in the presence of magnetic field and heat source, Int. J. Therm. Sci. 52 (2012) 161–175.
[32] M. Qasim, Heat and mass transfer in a Jeffrey fluid over a stretching sheet with heat source/sink, Alex. Eng. J. 52 (4) (2013) 571–575.
[33] Kalidas Das, Pinaki Ranjan Duari, Prabir Kumar Kundu, Nanofluid flow over an unsteady stretching surface in presence of thermal radiation, Alex. Eng. J. 53 (3) (2014) 737–745.
[34] Samir Kumar Nandy, Sumanta Sidui, Tapas Ray Mahapatra, Unsteady MHD boundary-layer flow and heat transfer of nanofluid over a permeable shrinking sheet in the presence of thermal radiation, Alex. Eng. J. 53 (4) (2014) 929–937.
[35] S. Das, R.N. Jana, Natural convective magneto-nanofluid flow and radiative heat transfer past a moving vertical plate, Alex. Eng. J. 54 (1) (2015) 55–64.
[36] Y.S. Daniel, S.K. Daniel, Effects of buoyancy and thermal radiation on MHD flow over a stretching porous sheet using homotopy analysis method, Alex. Eng. J. 54 (3) (2015) 705–712.
[37] P. Sudarsana Reddy, K.V. Suryanarayana Rao, MHD natural convection heat and mass transfer of Al_2O_3–water and Ag–water nanofluids over a vertical cone with chemical reaction, Proc. Eng. 127 (2015) 476–484.
[38] A.V. Kuznetstov, D.A. Neild, Natural convective boundary-layer flow of a nanofluid past a vertical plate: a revised model, Int. J. Therm. Sci. 77 (2014) 126–129.
[39] D.C. Venerus, J. Buongiorno, R. Christianson, J. Townsend, I. C. Bang, G. Chen, et al, Viscosity measurements on colloidal dispersions (nanofluids) for heat transfer applications, Appl. Rheol. 20 (2010) 445–482.
[40] E. ToolBox, Constant Pressure Heat Capacity of Water vs. Temperature. <http://www.engineeringtoolbox.com/water-thermal-properties-d_162.html>, 2013 (retrieved 01.11.13).
[41] E. ToolBox, Fuels, Densities and Specific Volumes Properties. <www.engineeringtoolbox.com/fuels-densities-specific-volumes-d_166.html>, 2013 (retrieved 01.11.13).
[42] S.D.B. Ceramaret, Physical mechanical thermal, electrical and chemical properties (2013).
[43] R. Bhargava, R. Sharma, O.A. Bég, Oscillatory chemically-reacting MHD free convection heat and mass transfer in a porous medium with Soret and Dufour effects: finite element modeling, Int. J. Appl. Math. Mech. 5 (2009) 15–37.
[44] O. Anwar Bég, H.S. Takhar, R. Bhargava, S. Rawat, V.R. Prasad, Numerical study of heat transfer of a third grade viscoelastic fluid in non-Darcian porous media with thermophysical effects, Phys. Scr. 77 (2008) 1–11.
[45] P. Rana, R. Bhargava, Flow and heat transfer of a nanofluid over a nonlinearly stretching sheet: a numerical study, Commun. Nonlinear Sci. Numer. Simul. 17 (2012) 212–226.